(1)

FINAL REPORT

STUDIES OF CUBIC ICE CRYSTALS

Grant Number: N00014-90-J-1187

William G. Finnegan and Richard L. Pitter

Atmospheric Sciences Center, Desert Research Institute

University of Nevada System

Reno, Nevada 89506

December, 1991

CONTENTS

REPORT DOCUMENTATION PAGE

Form Approved
OMB No. 0704-0188

1. AGENCY USE ONLY (Leave blank)	2. REPORT DATE	3. REPORT TYPE AND DATES COVERED
	12/91	Final 10 Oct 89 - 09 Oct 90

4. TITLE AND SUBTITLE
Studies of Cubic Ice Crystals

5. FUNDING NUMBERS
N00014-90-J-1187

6. AUTHOR(S)
William G. Finnegan and Richard L. Pitter

7. PERFORMING ORGANIZATION NAME(S) AND ADDRESS(ES)
Desert Research Institute
P.O. Box 60220
Reno, NV 89506

8. PERFORMING ORGANIZATION REPORT NUMBER

9. SPONSORING/MONITORING AGENCY NAME(S) AND ADDRESS(ES)
ONR RESIDENT REPRESENTATIVE
STANFORD UNIVERSITY
ROOM 202, McCULLOUGH BLDG.
STANFORD, CALIFORNIA 94305-4055

10. SPONSORING/MONITORING AGENCY REPORT NUMBER

11. SUPPLEMENTARY NOTES

12a. DISTRIBUTION/AVAILABILITY STATEMENT
Unlimited/unlimited

12b. DISTRIBUTION CODE

13. ABSTRACT (Maximum 200 words)
Report on factors that influence the shpaes of ice crystals growing in the atmosphere.

14. SUBJECT TERMS
ice crystals, atmospheric, stratoshperic chemistry

15. NUMBER OF PAGES
25

16. PRICE CODE

17. SECURITY CLASSIFICATION OF REPORT	18. SECURITY CLASSIFICATION OF THIS PAGE.	19. SECURITY CLASSIFICATION OF ABSTRACT	20. LIMITATION OF ABSTRACT
Unclas	Unclas	Unclas	Unlimited

GENERAL INSTRUCTIONS FOR COMPLETING SF 298

The Report Documentation Page (RDP) is used in announcing and cataloging reports. It is important that this information be consistent with the rest of the report, particularly the cover and title page. Instructions for filling in each block of the form follow. It is important to *stay within the lines* to meet *optical scanning requirements.*

Block 1. Agency Use Only *(Leave blank).*

Block 2. Report Date. Full publication date including day, month, and year, if available (e.g. 1 Jan 88). Must cite at least the year.

Block 3. Type of Report and Dates Covered. State whether report is interim, final, etc. If applicable, enter inclusive report dates (e.g. 10 Jun 87 - 30 Jun 88).

Block 4. Title and Subtitle. A title is taken from the part of the report that provides the most meaningful and complete information. When a report is prepared in more than one volume, repeat the primary title, add volume number, and include subtitle for the specific volume. On classified documents enter the title classification in parentheses.

Block 5. Funding Numbers. To include contract and grant numbers; may include program element number(s), project number(s), task number(s), and work unit number(s). Use the following labels:

C	- Contract	PR	- Project
G	- Grant	TA	- Task
PE	- Program Element	WU	- Work Unit Accession No.

Block 6. Author(s). Name(s) of person(s) responsible for writing the report, performing the research, or credited with the content of the report. If editor or compiler, this should follow the name(s).

Block 7. Performing Organization Name(s) and Address(es). Self-explanatory.

Block 8. Performing Organization Report Number. Enter the unique alphanumeric report number(s) assigned by the organization performing the report.

Block 9. Sponsoring/Monitoring Agency Name(s) and Address(es). Self-explanatory.

Block 10. Sponsoring/Monitoring Agency Report Number. *(If known)*

Block 11. Supplementary Notes. Enter information not included elsewhere such as: Prepared in cooperation with...; Trans. of...; To be published in.... When a report is revised, include a statement whether the new report supersedes or supplements the older report.

Block 12a. Distribution/Availability Statement. Denotes public availability or limitations. Cite any availability to the public. Enter additional limitations or special markings in all capitals (e.g. NOFORN, REL, ITAR).

- DOD - See DoDD 5230.24, "Distribution Statements on Technical Documents."
- DOE - See authorities.
- NASA - See Handbook NHB 2200.2.
- NTIS - Leave blank.

Block 12b. Distribution Code.

- DOD - Leave blank.
- DOE - Enter DOE distribution categories from the Standard Distribution for Unclassified Scientific and Technical Reports.
- NASA - Leave blank.
- NTIS - Leave blank.

Block 13. Abstract. Include a brief *(Maximum 200 words)* factual summary of the most significant information contained in the report.

Block 14. Subject Terms. Keywords or phrases identifying major subjects in the report.

Block 15. Number of Pages. Enter the total number of pages.

Block 16. Price Code. Enter appropriate price code *(NTIS only).*

Blocks 17. - 19. Security Classifications. Self-explanatory. Enter U.S. Security Classification in accordance with U.S. Security Regulations (i.e., UNCLASSIFIED). If form contains classified information, stamp classification on the top and bottom of the page.

Block 20. Limitation of Abstract. This block must be completed to assign a limitation to the abstract. Enter either UL (unlimited) or SAR (same as report). An entry in this block is necessary if the abstract is to be limited. If blank, the abstract is assumed to be unlimited.

LIST OF FIGURES

ONR IST/SDIO PROGRAM OVERVIEW

The Desert Research Institute (DRI) research program was organized to study factors that influence the shapes of ice crystals growing in the atmosphere. Although the Strategic Defense Initiative Organization (SDIO) Innovative Science and Technology (IST) Office's Middle Atmospheric Program (MAP) focused on stratospheric and mesospheric clouds, tropospheric clouds were also relevant to the utility and requirements of the ground-based laser program. In four years, the DRI research program contributed considerable advancements to understanding factors that influence ice crystal morphology, regulate microphysical processes of ice crystal initiation, growth, and interaction, and induce chemical oxidation or reduction reactions in atmospheric ice crystals by previously undocumented processes.

In this final year of the program, investigators focused on questions of ice crystal morphological behavior under various conditions, such as when they fall or rise into a temperature regime which is inconsistent with their existing habit. The literature is unclear on this question; most published results indicate that if the conditions change, the ice crystal will change its growth characteristics.

1. INTRODUCTION

Morphological features of ice crystals were first scientifically detailed in the 17th Century by the astronomer Johannes Kepler, yet even in the republication of that essay, Mason (in Kepler, 1966) conceded that not enough is presently known to answer the questions of why ice crystals assume the shapes they do.

Knowledge of how and why ice crystals grow to assume different shapes has value that extends beyond the realm of natural curiosity, with applications to a variety of topics, including radiative scattering (climate change), stratospheric chemistry (heterogeneous reactions occurring in the ozone hole), and laser penetration of ice clouds (SDIO).

2. THEORETICAL BASIS OF EXPERIMENTS

Finnegan and Pitter (1988) postulated the existence of electric multipoles on growing atmospheric ice crystals, having sufficient magnitude to affect the nature of ice crystal aggregation. Their postulate was reformulated as a hypothesis (Pitter and Finnegan, 1990) and tested by means of its effects on a variety of cloud microphysical processes, including aerosol scavenging (Pitter and Zhang, 1991), ice crystal morphology (Pitter and Finnegan, 1990), and secondary ice crystal formation (Pitter and Finnegan, 1990). More recently, Finnegan et al. (1991) demonstrated another, chemical aspect of the chemical ion separation that is hypothesized to occur at growing ice crystals, and because of the requirement in the chemical reactions that the salts be dissolved and ionized, also demonstrated unequivocally the existence of a liquid layer at growing ice surfaces of sufficient magnitude to dissolve and ionize salts.

The electric multipole concept of Finnegan and Pitter was derived from consideration of freezing potentials in bulk water freezing experiments, first conducted by Workman and Reynolds (1950) and later confirmed by a variety of investigators. In the bulk experiments, where freezing advanced in one direction, it was shown that the growing ice phase selectively incorporated some chemical ions, principally ammonium ion and the halide ions, at rates which were proportional to the rate of advance of the ice phase and which depended on the solute content in the aqueous phase. Experiments on freely-falling growing single ice crystals by the principal investigators have demonstrated that all these attributes of bulk freezing are applicable to atmospheric ice crystals. The evidence furthermore indicates that ion separation may be more rapid in growing ice crystals than in the bulk freezing case.

The separation of charge in growing ice crystals was hypothesized by Finnegan and Pitter to consist, essentially, of potential differences across each growing ice interface (Figure 1). Each interface may be idealized as an electric dipole, so the collective ensemble is generally termed an electric multipole. The net charge on the ice crystal (including the thin liquid layers at growing interfaces) due to the charge separations is zero, and in atmospheric cases there may exist, independent of the freezing potential, a net charge of either sign on the crystal, as a result of some ice crystal charging process.

The gross ice crystal shape, called its habit, is determined by the temperature and supersaturation of the environment in which it grows (Figure 2). No theoretical work has yet been able to unravel the question of why ice crystal habits change three times (plates-columns-plates-columns) between 0 and -20°C. Studies of ice crystal habit have principally been performed in isothermal chambers, and some apparently contradictory conclusions have arisen with regard to what shapes crystals take when they experience temperature changes that move them into a new growth regime. The question of habit changes in growing ice crystals is now being addressed.

3. EXPERIMENTAL

3.1 FACILITIES AND PROCEDURES

The experiments are conducted in the DRI 6.7 m^3 cloud chamber, which is operated at ambient pressure (about 850 mb). Initially, a supercooled liquid water cloud is generated by nebulization, as in prior studies (Finnegan and Pitter, 1988; Pitter and Finnegan, 1990; Finnegan *et al.*, 1991). Ultrasonic nebulization produces droplets about 10 μm radius with minimal electric charges. Ice crystals are nucleated by rapid expansion of moist compressed air, and grow principally by vapor diffusion in free fall until they settle to the chamber floor. The ice cloud exists in the 3 m high chamber for 7 to 20 minutes, depending on initial conditions. Ice crystals are sampled by collection on pre-

chilled, exposed glass microscope slides, which are removed for microscopic examination. Photomicrographs at 40X magnification document the size, habit, and detailed morphology of the ice crystals at 1 - 2 minute intervals during the run.

The cloud chamber temperature is manually controlled by adjusting two valves: the vapor return (suction) valve, which controls the volume of refrigerant cycled through the compressor; and the expansion valve, which controls the amount of cooling the refrigerant undergoes upon return from the compressors to the holding tank. The chamber also has limited computer control of temperature by adjusting the refrigerant expansion valve to maintain the average chamber air temperature to within 0.5 °C of a specified value at all times during the run. The chamber is sufficiently well controlled that the air temperature at any point in the chamber is always within 1°C of the average air temperature. The computer program also records temperatures, and will be upgraded to record photodetector readings.

The shape of the initial ice crystals formed during any run is determined by two parameters, the chamber air temperature and the salt content in the supercooled cloud drops, as described by Pitter and Finnegan (1990). The degree of ice crystal morphological detail is controlled by the freezing potential (viz., the electric potential across the ice-water interface) of the solution used in the cloud water, while the habit is a function of the temperature, supersaturation with respect to ice, and perhaps electric multipoles. For columnar ice crystals, the aspect ratio of the crystals is temperature-dependent, with short columns present at -7 to -8°C. The internal structure of columnar crystals depends on the freezing potential of the solution used in the cloud water. Deionized water forms more polyhedral crystals, while solutions with high freezing potential form skeletal crystals.

Similarly, plate-like crystals can be grown either as plates, as stellars with long, simple branches, or as various dendritic forms with secondary branching by selecting the temperature and by incorporating selected salts at parts per million concentrations in the ice crystals. Bullet rosettes are formed

in the cloud chamber by also controlling the mode of ice crystal formation. All these techniques are operational. The experiments generated ice crystals of controlled shape and morphology, so that the ice crystals closely resemble those in cirriform clouds. The ice crystals were sampled for photomicrographic documentation through the duration of the experiment, so researchers could determine the ice crystal shapes and size spectra throughout the experimental run.

3.2 CASES STUDIED

This section contains summaries of the cases studied on the variation in ice crystal habit and morphology during decreasing temperature, beginning either in the plate regime ($T > -4°C$) or in the column regime. These constitute a small fraction of cases conducted either with constant temperature or with temperature varying during the run. The summaries are taken from laboratory notes and may be tersely written in places.

3.2a Ammonium Chloride Solution Ice Crystals

The supercooled cloud was generated by ultrasonic nebulization of a dilute solution (10^{-4} N) of ammonium chloride, resulting in an estimated initial supercooled liquid water content of about 2 g m^{-3} (not measured). Ice was initiated by adiabatic expansion of moist compressed air in this set of experiments while the cloud chamber temperature was decreasing. Two runs were successfully conducted in this manner.

First experimental run

Seeding was initiated at -2.5°C and the temperature rose to -2.2°C at 1 minute before decreasing steadily to -7.8°C at 14 minutes.

Initially, all crystals observed were plates. At 7 minutes (-5.6°C), fewer than 5% of the crystals were columns. The maximum size was about 20 μm. At 9

minutes (-6.5°C), about 60% of the crystals were short columns, and moderate aggregation was noted despite all crystals being 20 µm or less in extent. At 12 minutes (-7.2°C), about 90% of the crystals were columns. A few crystals have reached 30 µm extent, and almost all were less than 20 µm across. At 14 minutes (-7.8°C), all the crystals were columns, and aggregation was moderate.

Second experimental run

Chamber temperature decreased from -4.2 to -6.7°C during the first six minutes, then varied by less than 0.5°C over the next 10 minutes, eventually decreasing to -8.8°C at 22 minutes. Thirteen photographs were taken during this period.

At 1 minute (-4.9°C), ice crystals were all small (<=30µm). About 80% were plates and 20% were columnar, mostly very thin (<10µm diam). About 20% of the plates were not simple, transparent plates, but contained internal structures, and about 10% of the plates were simple triangular crystals.

At 3 minutes (-6.0°C), the ice crystals did not differ noticeably from the previous photograph. At 4 minutes (-6.4°C), the ice crystals had similar shapes and sizes, but the columnar crystals had increased to about 30% of the total. At 5 minutes (-6.5°C), columnar crystals made up about 20% of the total. A cursory view of the crystals indicated slight diffusional growth of the population. (Perhaps a complete assay would have yielded quantitative results, but the uncertainty in crystal density, shape, and in some cases thickness prevented one from quantifying size.)

At 7 minutes (-6.7°C), about 75% of the crystals were columnar, varying from thick columns to thin, polyhedral columns. About 10% were simple plates (hexagonal and triangular), and the remainder were aggregated and difficult to discern with certainty. At 15 minutes (-6.6°C), all the crystals were columns, the larger ones with concave basal planes (needle-like extensions). Crystal sizes ranged up to 80 µm long and 20 µm diameter.

At 22 minutes (-8.8°C), most of the crystals remaining in the chamber were columns about 90 μm long and 50 μm diameter. Some exhibited a tendency for metamorphoses to capped columns, while others exhibited extensions of basal planes from interior regions (colloquially termed "axle rods,"). The internal structure of the columns indicated concave basal planes and suggested concave prism faces in at least one instance.

3.2b Ammonium Sulfate Solution Ice Crystals

The cloud was generated by ultrasonic nebulization of a dilute solution (10^{-4} N) of ammonium sulfate in deionized water. When the cloud chamber liquid water content was about 2 g m^{-3} (estimated) and the cloud chamber temperature was decreasing, ice was initiated by rapid adiabatic expansion of moist compressed air. The shapes and sizes of ice crystals falling onto glass microscope slides at various times were noted from microphotography. Three experimental runs were completed in this manner.

First experimental run

Seeding was somewhat premature, at -2.8°C while the temperature was rising. Temperature continued rising for 4 minutes, where it reached -1.6°C, then decreased to -3.5°C at 10 minutes.

Thin hexagonal plates predominated. Most crystals were aggregated (2 to 4 crystals per aggregate). One small, simple column appeared on the last slide. The slide at 2 minutes contained a crystal of 80 μm diameter, but the crystals at 10 minutes were all typically 50 to 60 μm diameter. The thickest plates that landed on the side had aspect ratios of 5:1. The warm temperature led to a low ice crystal formation rate, which was nevertheless sufficient for rapid aggregation to occur.

Second experimental run

The cloud was nucleated at -2.0°C and the temperature fell continuously and nearly uniformly for 13 minutes when it reached -6.9°C. The initial slide at 2 minutes (-2.6°C) showed simple plates up to 30 μm diameter and 10 μm thick. At 3 minutes (-2.8°C), thick plates were predominant but a few nearly isogonal columns and some very thin triangular plates were noted. Over half the crystals were aggregated.

At 8 minutes (-5.5°C), the crystal population on the slide appeared to be equally divided between thick plates and short columns, with a few more extreme specimens apparent. The maximum crystal dimension was less than 40 μm. Only about 10% of the crystals were aggregated. At 9 minutes (-6.1°C), columns up to 70 μm long and 30 μm wide predominated, often with narrower axles protruding from both (concave) basal planes. About 10% of the crystals were plates; about 10% of the crystals were aggregated.

Third experimental run

The cloud was nucleated at -2.4°C. The temperature continuously and steadily decreased to -6.4°C at 20 minutes. Initially, plates were exclusively found, with diameters to 30 μm. At 5 minutes (-4.5°C) some of the plates were nearly isogonal, and at 7 minutes (-5.0°C) about 30% of the crystals were columns. By 10 minutes (-5.4°C), the majority of crystals were columns.

From 10 to 20 minutes, the temperature decreased only to -6.4°C. The crystals at 15 minutes (-5.9°C) were moderately aggregated hollow columns, some with internal axles. Their lengths approached 100 μm and their widths were as large as 20 to 30 μm.

At 17 minutes (-6.1°C), the number concentration of ice crystals had significantly diminished in the chamber. A columnar crystal about 90 μm long and 60 μm diameter was photographed with strongly concave basal planes and a 10μm fluting banding the prism faces at each basal plane.

3.2c Sulfuric Acid Solution Ice Crystals

The supercooled liquid water cloud was formed by ultrasonic nebulization of a dilute solution (10^{-4} N) of sulfuric acid in deionized water. When the liquid water content was about 1 - 2 g m^{-3} (not measured) and the chamber temperature was decreasing, ice was initiated by rapid expansion of moist compressed air. Two experimental runs were conducted in this manner.

First experimental run

Seeding was performed at -1.3°C, but the temperature rose to -0.5°C at 2 minutes before decreasing. Because very few crystals were nucleated, a second seeding was performed at 11 minutes at -2.3°C.

Columns were first observed at -4°C (20 minutes), and were the dominant habit at -4.3°C (24 minutes). At 26 minutes (-4.5°C), about 70% of the crystals were simple columns and the rest were simple, thick plates. At 28 minutes (-5.0°C), some of the columns had developed modest concave basal planes and several crystals had noticeable twinning lines. At 29 minutes (-5.4°C), needles over 100 μm long appeared, some with concave basal planes and a few with internal axles. The thicker columns still appeared on the slide.

Second experimental run

The cloud was seeded at -2.6°C and again 4 minutes later (-3.1°C). The temperature decreased slowly to -5.3°C at 20 minutes. At 10 minutes (-3.4°C), the ice crystals were predominantly plates, with fewer than 10% of the crystals being columns. At 15 minutes (-4.6°C), most of the ice crystals were nearly isogonal, and columns and plates appeared to be about equally present. At 16 minutes (-4.7°), longer simple columns appeared and columns made up about 60% of the total. At 20 minutes (-5.3°C), a few columns still existed, ranging from 60 to 300 μm long. The larger columns had concave basal planes and some had axles.

3.3 DISCUSSION

The experimental results indicate that ice crystals that grow continuously in a supercooled liquid water cloud do not change their fundamental habit during growth, but that hybrid habit crystals (tsunamis) evolve during runs which experience excessive cooling.

Studies of ice crystal morphology during diffusion growth in an environment undergoing temperature change have yielded much information about ice crystal behavior in these environments. It was found that ice crystals don't change their mode of growth just because they fall into a different growth regime; they continue growing with their original morphological characteristics, at least for awhile. As the growth continues in a cooling environment, the increased mass and heat fluxes make the crystal morphology more elaborate. That is, columns tend to develop fluted ends or even into capped columns, and secondary columnar growth, in the form of axles, arise. This appears to be a tendency to maximize the crystal's radiating area so it can accept the available moisture.

In contrast, studies conducted with rising temperatures generally yielded no differences in crystal morphology with time, although the growth rates of the crystals appeared to be much slower.

The experimental procedure allowed us a glimpse at ice crystal formation (generally called nucleation, but we distinguish between the very rapid process that creates the initial stable ice phase and the more tangible processes which lead to the formation of visible ice crystals). The compressed air gun causes adiabatic expansion of a small volume of compressed, moist room temperature air. The adiabatic expansion cools the air to below -40°C before mixing and heat transfer can raise the temperature back to cloud chamber ambient temperature. In that short time frame, we have postulated that many thermodynamically stable ice embryos are formed. A stable ice embryo can contain as few as perhaps 50 water molecules, and initially be as small as about 10-15 Angstroms diameter. These embryos have large diffusivities, and consequently initially contact, and

freeze, many supercooled (10 μm diameter) droplets in the vicinity of the expansion. The initial ice crystal population then consists of those drops that initially froze. The habit is set as the droplets freeze, and the morphology of the crystal is constant, under isothermal conditions, until it grows to a size larger than about 400 μm (and thus achieves a morphological instability of sorts).

Those embryos that did not initially freeze drops find a much reduced drop population on which to act, and hence the delayed droplet freezing rate is low. Experimental procedures sometimes allow a continual supply of supercooled drops to the chamber, and other times turn off the droplet supply at seeding. The effects of delayed droplet freezing are apparent by comparison of the ice crystal populations with time. Embryos that do not contact droplets grow by diffusion, but their mass growth rate is initially very slow due to their extremely small size. They need to grow to perhaps 0.1 μm diameter (larger than the mean free path of a water molecule) before they can effectively grow by diffusion.

This postulate is consistent with the experimental data collected thus far, and may provide the means for investigating stratospheric and mesospheric ice crystal formation mechanisms, but it requires additional testing and formulation of testable hypotheses.

4. THEORY OF ICE CRYSTAL HABIT

The work performed by the investigators on determining ice crystal habit, from fundamental concepts, is incomplete, but it still yields interesting and previously unpublished results of note. Its development was not in the research plan of the ONR study, nor in any other research plan. Its development was thus jointly funded by the ONR study, a grant from NOAA, a grant from NSF, and internal support.

4.1 INTRODUCTION

Ice crystal diffusion growth has been theoretically approached by several researchers, as detailed in Pruppacher and Klett (1978). The most successful attempts to date have applied the electrostatic analogy (McDonald, 1963) to determine the rate of ice crystal mass increase when ambient conditions and the ice crystal geometry were specified (Koenig, 1971; Jayaweera, 1971).

The electrostatic analogy theory is incomplete. The theory assumes that the vapor density and temperature fields about the crystal conform to the shape of the electric potential field about a conducting body of the same shape as the crystal, which imposes the assumption that the ice crystal surface is isothermal. We present theoretical arguments to the contrary, and present a model of ice crystal diffusional growth in the atmosphere which determines not only tne rate of mass increase, but also the rates of increase of the principal ice crystal axes. Thus, the theory addresses ice crystal habit as a consequence of ice crystal diffusional growth.

The fundamental theory of ice crystal habit has eluded researchers. Various mechanisms have been postulated, but it is difficult to formulate hypotheses which may be tested. Mason et al. (1963) argued that the step growth rate was a function of step height, and also a function of the collection distance a step could pick up a water molecule on the surface. The concept advanced was that basal and prism faces on crystals had different molecular migration distances, which varied unevenly with temperature. In contrast, Hobbs and Scott (1965) argued that vapor migration speed, rather than migration distance, was the mechanism for determining habits of ice crystals. Lamb and Hobbs (1971) discussed growth rates and habits of ice crystals, using a model of linear growth rates of different faces varying differently with different temperatures, and Lamb and Scott (1972) described an experiment that obtained linear growth rates of different ice crystal surfaces. Finally, Kuroda and Lacmann (1982) developed a theory of liquid-quasiliquid-solid (L-QL-S) growth on ice surfaces and postulated the effect of such on habit transition at different temperatures.

4.2 MODEL SPECIFICATION

We simplified the initial model development by making assumptions that could be investigated in more detail later. The ice crystal was specified as a right regular hexagonal prism (see Figure 3) of density ρ_I. Thus, two variables, a and c, determine the crystal mass and shape. This model was used to see whether consideration of details of heat and mass transport are sufficient to determine the ice crystal shape as well as its mass.

If an ice crystal is not isothermal, the simplest model of a crystal is one with basal faces of one temperature, T_B, and prism faces of another, T_P. The model of diffusion growth assumes that vapor flux to the crystal surface is proportional to the local vapor density gradient, the surface vapor density being defined as that at equilibrium with ice at the surface temperature. The condensation of vapor on the surface is accompanied by release of latent heat of condensation on the same crystal face. Condensed water may move from one face to another, but the total rate of condensation equals the total rate of freezing. Latent heat of freezing is released on the crystal face where freezing occurs. The local mass and thermal balances are then worked out separately for the basal and prism faces, and integrated crystal equations are similarly derived as constraints for the problem.

The initial model development ignores several processes that affect the local heat balance. These are the radiation term, the heat conduction through the crystal lattice from the warmer to the cooler faces, and the sensible heat transfer as condensate moves from a cooler condensing surface to a warmer freezing surface. The lattice term and the condensate term are directed in opposite directions, and the radiation term is small compared to the other terms in the energy balance equation.

4.3 GOVERNING EQUATIONS

In order to develop the equations for diffusion growth to a crystal with possibly different face temperatures, we begin with a review of the development of diffusion growth using electrostatic analogy theory.

4.3a Isothermal Crystal Development

When the ice crystal surface is isothermal, then the electrostatic analogy can be applied for vapor and heat diffusion to and from the crystal surface. The resulting relations are:

$$\frac{dQ}{dt} = 4\pi C K (T_s - T_\infty) \tag{1}$$

and

$$\frac{dM}{dt} = 4\pi C \mathcal{D} (\rho_\infty - \rho_i(T_s)) \tag{2}$$

In Eq. 2, the vapor density is expressed as vapor pressure by using the equation of state:

$$\frac{dM}{dt} = \frac{4\pi C \mathcal{D}}{R_v T_\infty} \left(e_\infty - \frac{T_\infty}{T_s} e_i(T_s) \right) \tag{3}$$

The Clasius-Clapeyron equation eliminates the vapor pressure at the crystal surface.

$$\frac{dM}{dt} = \frac{4\pi C \mathcal{D}}{R_v T_\infty} \left(e_\infty - e_i(T_\infty) \exp\left\{ \frac{L_s (T_s - T_\infty)}{R_v T_s T_\infty} \right\} \right) \approx \frac{4\pi C \mathcal{D} e_i(T_\infty)}{R_v T_\infty} \left[S_i - 1 - \frac{L_s (T_s - T_\infty)}{R_v T_\infty^2} \right] \tag{4}$$

Since the source of heat to be dissipated is latent heat,

$$\frac{dQ}{dt} = L_s \frac{dM}{dt} \tag{5}$$

Eliminating T_s by applying Eqs. 1 and 5 into Eq. 4, we obtain

$$\frac{dM}{dt} = \frac{4\pi C (S_i - 1)}{\left[\frac{R_v T_\infty}{D e_i(T_\infty)} + \frac{L_s^2}{K R_v T_\infty}\right]} \tag{6}$$

In the isothermal surface case, Pitter (1981) found that the vapor mass arrives at the surface of a crystal modeled as a oblate or prolate spheroid in such a manner that, if no migration occurs on the surface, the initial aspect ratio of the crystal is preserved. Moreover, it was shown that even with ventilation, the initial aspect ratio is preserved within a few percent.

4.3b Non-Isothermal Considerations

When T_B and T_P are not necessarily equal, we can develop equations of mass and heat balance on the basal and prism faces independently, and apply overall crystal balance equations.

Extending the results of Pitter (1981), we postulate that an isothermal hexagonal prism acquires vapor in a manner that preserves its initial aspect ratio. Thus, the aspect ratio H remains constant during growth, which leads to the relation

$$H = \frac{dc/dt}{da/dt} \Rightarrow c\frac{da}{dt} = a\frac{dc}{dt} \tag{7}$$

To first order accuracy, the mass growth rate on a basal face is

$$\left.\frac{dM}{dt}\right|_B = \frac{3\sqrt{3}}{2}\rho_I a^2 \frac{dc}{dt} \tag{8}$$

and that on a prism face is

$$\left.\frac{dM}{dt}\right|_P = \sqrt{3}\,\rho_I a c \frac{dc}{dt} \tag{9}$$

which indicates that each basal face receives 1.5 times the mass of each prism face. Of interest, this relationship is independent of crystal habit.

To apply this concept to a crystal with different surface temperatures, we postulate that each crystal surface grows as though it were on an isothermal crystal, and that the relative partitioning of mass among faces, as exemplified in Eqs. 8 and 9, applies. This postulate lets us keep the electrostatic capacitance factor. Because of local gradients near the crystal edges where basal and prism faces meet, we expect that this postulate has a small error. The postulate slightly reduces mass flux to the warmer surface and slightly increases mass flux to the cooler surface.

Heat transfer in the non-isothermal crystal case is postulated by analogy to be congruent with mass transfer as just described.

For a basal face, the right-hand sides of Eqs. 1 and 2 are multiplied by 1/6 and T_g is used instead of T_s. For a prism face, the right-hand sides of Eqs. 1 and 2 are multiplied by 1/9 and T_p is used instead of T_s.

If water mass does not migrate from one surface to the other (viz. isothermal crystal surface), the resulting growth rate is identical to Eq. 6. If water mass condenses on one surface and moves to another surface to freeze, then different theoretical development is needed, as follows.

The latent heat released on a crystal face is due to condensation and freezing, according to

$$\left.\frac{dQ}{dt}\right|_x = L_v \left.\frac{dM_c}{dt}\right|_x + L_f \left.\frac{dM_f}{dt}\right|_x \qquad (10)$$

where x refers to either the basal or prism face. The rates of freezing on the various faces are kinetically determined, neglecting second-order terms by Eqs. 8 and 9, substituting dM_f/dt for dM/dt in those equations.

We now derive the rate of mass condensation, dM_c/dt, for one basal face. Following the discussion above, the right-hand side of Eq. 2 is multiplied by 1/6 and the usual substitutions are made to yield

$$\left.\frac{dM_c}{dt}\right|_B = \frac{1}{6}\,\frac{4\pi D e_i(T_\infty)}{R_v T_\infty}\left[S_i - 1 - \frac{L_s(T_B - T_\infty)}{R_v T_\infty^2}\right]. \tag{11}$$

The temperature difference in the last term in the numerator is eliminated using Eq. 1 (again, with its right-hand side multiplied by 1/6). dQ/dt is eliminated using Eq. 10, which is appropriate for a single crystal face, yielding

$$\left.\frac{dM_c}{dt}\right|_B = \frac{1}{6}\,\frac{4\pi C(S_i - 1)}{(F_1 + F_2)} - \frac{F_3\,\frac{3\sqrt{3}}{2}\,\rho_I\,a^2\frac{dc}{dt}}{(F_1 + F_2)} \tag{12}$$

where

$$F_1 = \frac{R_v T_\infty}{D e_i(T_\infty)} \tag{13}$$

$$F_2 = \frac{L_s L_v}{K R_v T_\infty^2} \tag{14}$$

and

$$F_3 = \frac{L_s L_f}{K R_v T_\infty^2} \tag{15}$$

Similarly, the mass condensation rate on a prism face is derived as

$$\left.\frac{dM_c}{dt}\right|_P = \frac{1}{9}\,\frac{4\pi C(S_i - 1)}{(F_1 + F_2)} - \frac{F_3\,3\sqrt{3}\,\rho_I\,a\,c\,\frac{da}{dt}}{(F_1 + F_2)} \tag{16}$$

By summing the mass condensation on two basal faces and six prism faces, we get the total rate of mass condensation to the ice crystal.

$$\left.\frac{dM_c}{dt}\right|_{Total} = \frac{4\pi C(S_i - 1)}{(F_1 + F_2)} - \frac{F_3\,3\sqrt{3}\,\rho_I\left(a^2\frac{dc}{dt} + 6ac\frac{da}{dt}\right)}{(F_1 + F_2)} \tag{17}$$

Since the rate of mass increase is given by

$$\left.\frac{dM_c}{dt}\right|_{Total} = \left.\frac{dM_f}{dt}\right|_{Total} = 3\sqrt{3}\,\rho_i\left(2ac\frac{da}{dt} + a^2\frac{dc}{dt}\right) \tag{18}$$

we eliminate the da/dt term on the right-hand side of Eq. 18. After some algebraic manipulations, we have

$$\left.\frac{dM_c}{dt}\right|_{Total} = \frac{4\pi C(S_i - 1) - F_3 \cdot 12\sqrt{3}\,\rho_i\, ac\frac{da}{dt}}{F_1 + F_4} \tag{19}$$

where, as in the isothermal derivation, we get

$$F_4 = \frac{L_s^2}{KR_v T_\infty^2}. \tag{20}$$

The effect of different face temperatures on the growth rate is therefore manifested in a slight retardation term, which is proportional to the rate of growth along the a-axis. Hence, ice crystals with larger products ac da/dt have, by virtue of their temperature structures, slower growth rates.

In the extreme, we consider a crystal with da/dt=0. This eliminates the retarding term, but carried to extreme this results in very low values of C. On the other hand, a very thin plate minimizes the retarding product with a low value of c, while C for very thin plates approaches a minimum value of about 0.6. Another consideration is the thick plates or thick columns where a and c are nearly identical, and da/dt is approximately equal to dc/dt. This situation, close to the isothermal situation, has a maximum retarding effect. Comparing Eq. 19 with Eq. 6 (the isothermal case), we see that Eq. 19 has a retarding effect that Eq. 6 does not contain. We have not been able to explain the origin of this term--for an isothermal case, it should go to zero, but that is not the case (cf. Eq. 7).

4.4 SUMMARY OF THEORY TO DATE

The theory of ice crystal habit is incomplete, but it is significantly different in approach than any previous attempts to explain why ice crystals grow in different shapes at different temperatures. Previous attempts have investigated effective molecular migration distances or the speeds of molecular migration on different faces of the crystal. The experiments in support of those theories were conducted in the laboratory with ice crystals growing on substrates. This theory treats the detailed heat and mass transport about the crystal and shows, even in its incomplete state, that plates and columns can be viewed as having bare ice faces and liquid covered faces. The initial mechanism which causes some faces to become bare is yet to be determined.

5. SUMMARY AND CONCLUSIONS

The experiments and theoretical development undertaken in support of the IST/SDIO research program are oriented toward obtaining a fundamental understanding of the processes and mechanisms which determine the shapes of atmospheric ice crystals. It is only with such a level of understanding that scientists will be able to answer such questions as radiative scattering by different types of ice clouds in the atmosphere.

Experimentally, we extended our prior results (Pitter and Finnegan, 1990), which demonstrated that ice crystal morphology--the detailed shapes as opposed to the overall aspect ratio, which is known as the habit--is strongly influenced by included soluble ions. Furthermore, the degree of elaborateness of the crystal, which we have tentatively come to express as the ratio of perimeter to diameter, appears to be directly related to (perhaps even proportional to) the magnitude of the freezing potential. Extending this concept in the present study, we investigated the morphological (and habit) behavior of crystals growing in environments that were undergoing temperature changes. The purpose of these experiments was principally to determine the degree of "memory" a growing crystal has for its natal environment.

This experimentation also supports our concept of growing ice crystal charge separation, created through electric potentials acting across growing ice/water interfaces (and hence, the existence of liquid layers at least on the growing faces of atmospheric ice crystals). If a geometric configuration of bare and liquid-coated faces has developed in a growing crystal, then when the crystal falls into a different temperature regime, the geometric configuration provides a degree of inherent memory of its previous state. Until something causes either all the liquid coatings to freeze or all the surfaces to acquire liquid coatings, the ice crystal growth, though perhaps proceeding at a different rate, will continue to proceed with the same morphological characteristics.

Consistent with our experimental thrust, a theoretical initiative was undertaken to investigate the detailed roles of bare and liquid-coated crystal faces (and hence the overall concept of the role of electric multipoles in growing ice crystals) on determination of ice crystal habit. The theory has not yet been developed to a final, habit-determining point. Most notably, the electrical forces have not yet been included.

However, the theory does promise ability to consider the detailed heat and mass transfers about a growing ice crystal, treating either the two basal planes or the six prism faces as bare ice and the remaining faces as having a thin liquid coating. At present, there is no temperature-dependent term, which will ultimately be necessary for specification of a-axis or c-axis growth, and the initial aspect ratio appears to be conserved during growth.

Additional theoretical work is necessary in order to achieve a fundamental understanding of the forces involved in ice crystal habit. However, even the simple theoretical framework, established by restricting the crystal to a regular hexagonal prism, appears sufficiently detailed to advance our state of knowledge. It is important that the theoretical development use fundamental, well-understood concepts such as heat and mass transport properties, and be sufficiently detailed and accurate to specify how crystals behave under specific conditions, including (eventually) time-dependent ambient temperature. It is also essential that the

theory is capable of reproducing observations, and to that end it is necessary to continue an experimental task in support of this project.

REFERENCES

Finnegan, W.G., and R.L. Pitter 1988: A postulate of electric multipoles in growing ice crystals: Their role in the formation of ice crystal aggregates. *Atmos. Res.*, 22, 235-250.

Finnegan, W.G., R.L. Pitter, and L.G. Young 1991: Preliminary study of coupled oxidation-reduction reactions of included ions in growing ice crystals. *Atmos. Environ.*, 25A, 2531-2534.

Hobbs, P.V., and W.D. Scott, 1965: A theoretical study of the variation of ice crystal habits with temperature. *J. Geophys. Res.*, 70, 5025-5034.

Jayaweera, K.O.L.F., 1971: Calculations of ice crystal growth. *J. Atmos. Sci.*, 28, 728-736.

Kepler, J., 1966: *The Six-Cornered Snowflake.* Trans. and ed., C. Hardy. Oxford Clarendon Press, 74pp.

Koenig, L.R., 1971: Numerical modeling of ice deposition. *J. Atmos. Sci.*, 28, 226-237.

Kuroda, T., and R. Lacmann, 1982: Growth kinetics of ice from the vapour phase and its growth forms. *J. Crystal Growth*, 56, 189-205.

Lamb, D., and W.D. Scott, 1972: Linear growth rates of ice crystals grown from the vapor phase. *J. Crystal Growth*, 12, 21-31.

Lamb, D., and P.V. Hobbs, 1971: Growth rates and habits of ice crystals grown from the vapor phase. *J. Atmos. Sci.*, 28, 1506-1509.

Mason, B.J., G.W. Bryant, and A.P. Van den Heuvel, 1963: The growth habits and surface structure of ice crystals. *Phil. Mag., Ser. B*, 8, 505-526.

McDonald, J.E., 1963: Use of electrostatic analogy in studies of ice crystal growth. *Z. Angew. Math Phys.*, 14, 610-619.

Pitter, R.L., 1981: Convective diffusion and ice crystal habit. *J. Rech. Atmos.*, 14, 281-288.

Pitter, R.L., and W.G. Finnegan, 1990: An experimental study of effects of soluble salt impurities on ice crystal processes during growth. *Atmos. Res.*, 25, 71-88.

Pitter, R.L., and R. Zhang, 1991: Numerical simulation of the scavenging rates of ice crystals of various microphysical characteristics. *Adv. Atmos. Sci.*, 8, 175-200.

Pruppacher, H.R., and J.D. Klett, 1978: *Microphysics of Clouds and Precipitation*. Reidel, 714 pp.

Workman, E.J., and S.E. Reynolds, 1950: Electrical phenomena occurring during the freezing of dilute aqueous solutions and their possible relationship to thunderstorm electricity. *Phys. Rev.*, 78, 254-259.

FIGURE 1

Visualization of charge distributions in variously-shaped ice crystals

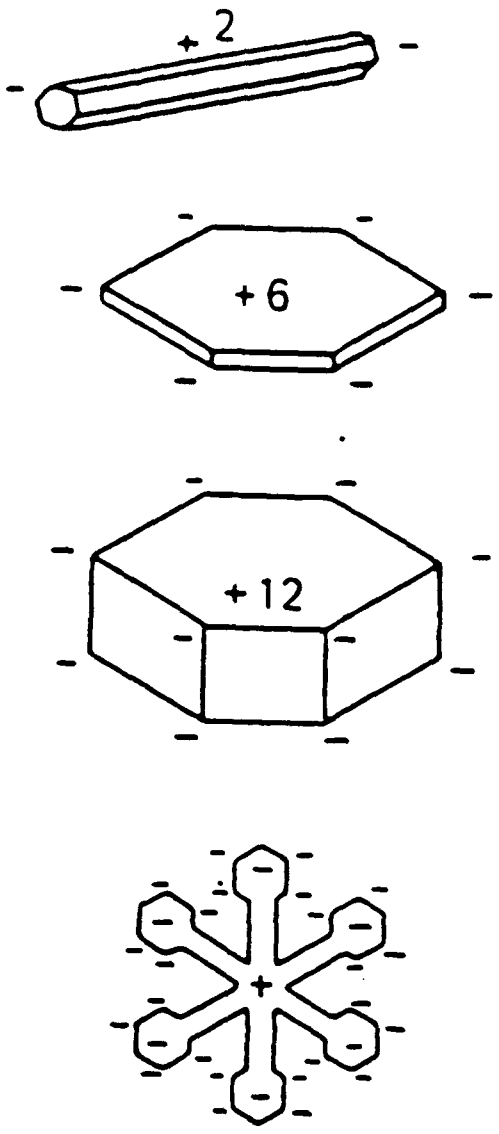

FIGURE 2

Temperature-Vapor density phase diagram of ice crystal habits

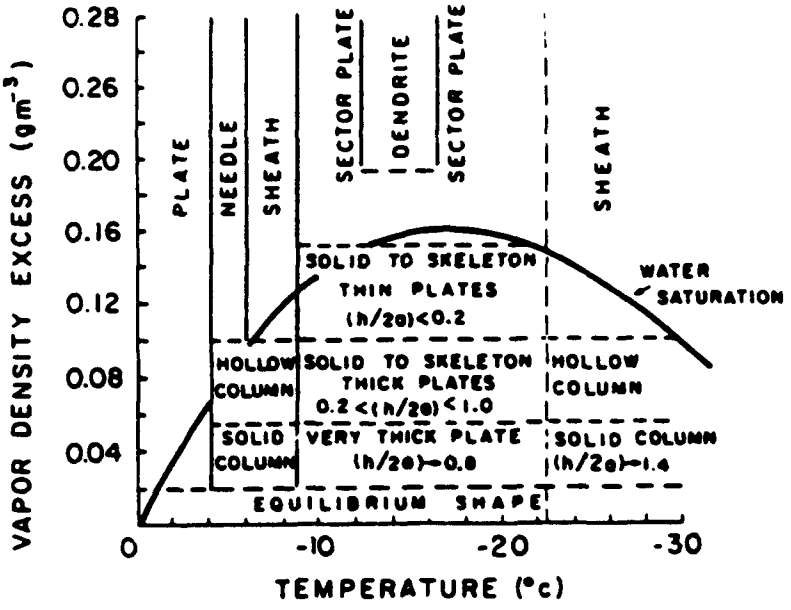

Variation of ice crystal habit with temperature and vapor density excess. (Based on laboratory observations of Kobayashi, 1961; and Rottner and Vali, 1974.)

FIGURE 3

Model ice crystal for use in derivation of ice crystal habit

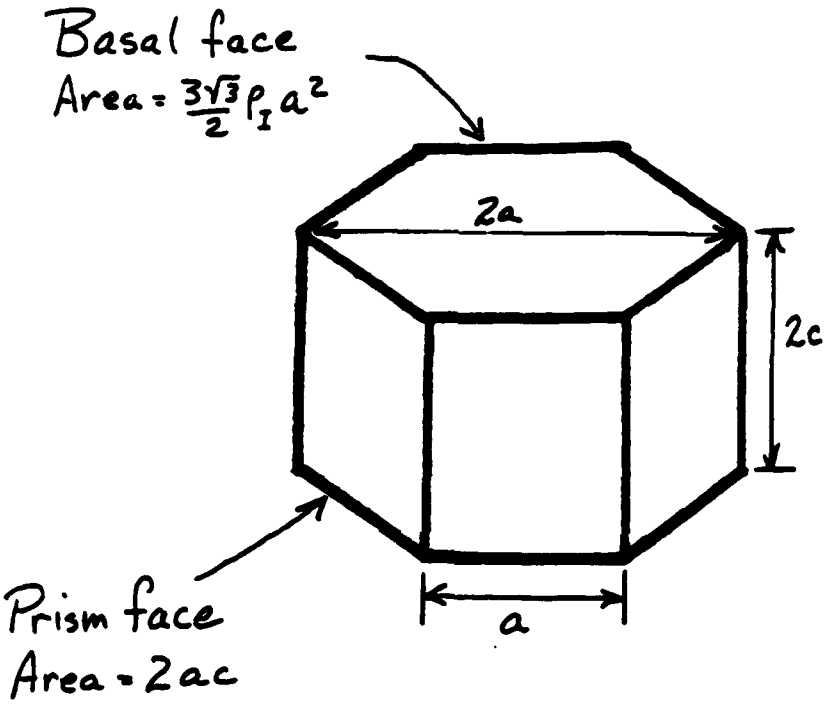

Crystal Volume = $3\sqrt{3}\,a^2c$

Aspect Ratio = c/a